

Many-body carrier interaction effects in quantum wells

Alfred Kahan and Lionel Friedman

Rome Laboratory, Optics Technology Division, Hanscom AFB, Bedford, Massachusetts 01731

(Received 4 October 1996)

Many-body carrier interaction effects shift the ground- and excited-state subband energy levels of quantum wells. We derive carrier-carrier Coulomb exchange and direct interaction energies as a function of carrier density, quantum well composition, and well width. For values of these parameters of physical interest, the excited-state exchange energy is small compared to the ground-state exchange energy. Our expressions for the ground- and excited-state direct interactions yield considerably smaller energy values than those reported by previous investigators. This is due to the fact that in our derivations we differentiate between quantum well width, carrier doping width, and ground- and excited-state wave function effective confinement lengths. Direct interaction energies increase linearly with carrier density, and for large carrier densities substantially negate exchange interaction effects. We illustrate carrier-carrier interaction effects for the heavy-hole subband of electrically neutral, p -type, isolated strained-layer $\text{Ge}_x\text{Si}_{1-x}/\text{Si}$ quantum wells. [S0163-1829(97)05608-7]

I. INTRODUCTION

In a series of publications, Coon and co-workers evaluated many-body interaction effects on ground- and excited-state energy levels of doped quantum wells.¹⁻⁶ Specifically, they evaluated the Coulomb direct and exchange interaction energies. Direct interaction energies are positive and raise $E(\text{hh}_0)$ and $E(\text{hh}_1)$, the heavy-hole ground- and excited-state energies in the absence of interaction, to higher energies. The exchange energies are negative and shift $E(\text{hh}_0)$ and $E(\text{hh}_1)$ to lower energies. The net carrier density induced energy shift, $\Delta E(\text{cc})$, is a balance between these positive and negative shifts.

In Refs. 1 and 2, Bandara and Coon formulate Hartree-Fock equations for Coulomb direct and exchange interactions, and solve for the ground- and excited-state direct and exchange interaction energies, E_{dir}^0 , E_{dir}^1 , E_{ex}^0 , and E_{ex}^1 , respectively. In deriving E_{ex}^0 they approximate an exponential by the first two terms, and in deriving E_{ex}^1 they approximate an exponential by the first nonvanishing term of its power series expansion. It is claimed that in this approximation E_{ex}^1 is small compared to E_{ex}^0 . However, for an electrically neutral doped quantum well, they show that $E_{\text{dir}}^1/E_{\text{dir}}^0 = \frac{2}{3}$, so transition energy calculations do have to consider the upper-state direct interaction energy.

In Ref. 3, Choe *et al.* derive E_{ex}^0 , but not E_{ex}^1 , based on the complete series expansion of the exponential. The authors also note that the length to be used calculating E_{ex}^0 is the confinement length L'_0 , the length at which the ground-state wave function of the quantum well extrapolates to zero in the barrier region. However, the authors did not correct E_{dir}^0 for L'_0 . In Ref. 4, Choe *et al.* refine the mathematics of Ref. 3. In Ref. 5, a review paper, the authors formulate interaction effects based on derivations of Refs. 1 and 2. Reference 6 is the Ph.D. thesis of Bandara. Thus, in their treatment of many-body interactions, exchange and direct Coulomb interaction effects are not treated in a systematic manner. One missing element is E_{ex}^1 , based on the full expansion of the exponential. Another element is that they derive E_{dir} based on the well width L , and neglect the consid-

erable effects of the confinement lengths. E_{dir}^0 and E_{dir}^1 increase linearly with carrier density, and for large carrier densities ($E_{\text{dir}}^1 - E_{\text{dir}}^0$) may substantially negate E_{ex}^0 .

In this investigation we follow and extend the formalism outlined by Coon *et al.*, and derive E_{ex}^0 based on the complete power series expansion of the exponential. The specific format of our series solution is more convenient to apply, and we obtain identical numerical results. Similarly, we derive E_{ex}^1 based on the fully expanded exponential. We find, in agreement with Coon and co-workers, that E_{ex}^1 is small compared to E_{ex}^0 . In many practical devices, the carrier doping width is smaller than the quantum well width. In our derivations we distinguish between quantum well width, doping width, and ground- and excited-state wave function confinement lengths. We find that by appropriately applying these different lengths, our equations for the direct interaction mechanism yield considerably smaller E_{dir}^0 and E_{dir}^1 values than the ones derived by the previous investigators. Our equations reduce to earlier results if all lengths are taken to be identical. We illustrate our carrier density results for the heavy-hole subband of electrically neutral, p -type, isolated strained-layer, $\text{Si}_{1-x}\text{Ge}_x/\text{Si}$ quantum wells.

II. EXCHANGE INTERACTION

The Coulomb exchange potential V_{ex} of a carrier in state i due to carriers in all possible states j , Ref. 1, is

$$V_{\text{ex}}^i(\mathbf{r}) = \frac{e}{4\pi\epsilon} \sum_j \int d\mathbf{r}' \frac{1}{|\mathbf{r}-\mathbf{r}'|} \psi_j^*(\mathbf{r}') \psi_i(\mathbf{r}'), \quad (1)$$

and the exchange interaction energy is

$$\begin{aligned} E_{\text{ex}}^i(\mathbf{r}) &= -e \int d\mathbf{r} \psi_i^*(\mathbf{r}) V_{\text{ex}}^i(\mathbf{r}) \psi_j(\mathbf{r}) \\ &= -\frac{e^2}{4\pi\epsilon} \sum_j \int d\mathbf{r} \int d\mathbf{r}' \frac{1}{|\mathbf{r}-\mathbf{r}'|} \psi_j^*(\mathbf{r}') \psi_i(\mathbf{r}') \\ &\quad \times \psi_j(\mathbf{r}) \psi_i^*(\mathbf{r}). \end{aligned} \quad (2)$$

For the ground state, $i=0$. Here e is the electronic charge, ϵ is the dielectric constant, and $\psi_j(\mathbf{r})$ are the basis functions of

a carrier in state j . Exchange interaction energies are negative, and lower $E(\text{hh}_0)$ and $E(\text{hh}_1)$, the heavy-hole subband ground- and excited-state energy levels of an undoped quantum well. This mechanism increases the intersubband transition energy (blueshift).

The basis functions are

$$\psi_n(\mathbf{r}) = \frac{1}{A^{1/2}} \exp(i\mathbf{k}_n \cdot \mathbf{s}) \phi_0(x). \quad (3)$$

We choose the origin of the normalized ground-state one-electron wave function, $\phi_0(x)$, to be at the quantum well center,

$$\phi_0(x) = \sqrt{2/L'_0} \cos(k_0 x), \quad |x| < L'_0/2 \quad (4)$$

where $k_0 = \pi/L'_0$. In these equations \mathbf{s} is a two-dimensional position vector in the heterostructure plane, x is a one-dimensional displacement normal to the quantum well plane, \mathbf{k} is a two-dimensional wave vector parallel to the well, and A is the quantum well lateral area. The ground-state confinement length L'_0 is the length at which the ground-state envelope function penetrating into the barrier region extrapolates to zero.

The maximum carrier induced energy shift occurs at the zone center, at wave vector $k=0$. Following the procedures outlined in Ref. 3, E_{ex}^0 , at $k=0$, is

$$E_{\text{ex}}^0(k=0) = -\frac{e^2}{4\pi\epsilon_0} \frac{k_F}{\epsilon_r} f^0(\beta)_{k=0}, \quad (5)$$

where $f^0(\beta)_{k=0}$ is given by

$$\begin{aligned} f^0(\beta)_{k=0} &= \sum_{n=0}^{\infty} \frac{(-1)^n}{(n+1)} \beta^n \pi^n \left\{ \frac{2}{(n+2)!} - \frac{1}{(2\pi)^{n+1}} \sin(n\pi/2) \right. \\ &+ \frac{3}{(2\pi)^{n+2}} \cos(n\pi/2) - \sum_{k=0}^n \frac{1}{(2\pi)^{k+2}} \frac{1}{(n-k)!} \\ &\left. \times \left[\frac{2\pi k}{(n+1-k)} \sin(k\pi/2) + 3 \cos(k\pi/2) \right] \right\}. \quad (6) \end{aligned}$$

The parameter β is

$$\beta = k_F/k_0. \quad (7)$$

The radius of the two-dimensional Fermi sea is $k_F = (2\pi\sigma)^{1/2}$. Here, $\sigma = N_D L_d$ is the carrier sheet density, N_D is the ionized impurity density, and the doping width is L_d , which can be smaller than the well width L . Assuming complete ionization, the carrier concentration is taken to be equal to the impurity concentration. We designate N_D as the carrier density, implying either donors or acceptors. Also, $\epsilon = \epsilon_0 \epsilon_r$, where ϵ_0 and ϵ_r are the dielectric constants of free-space and well material, respectively. The specific format of Eq. (6) differs from the one given in Ref. 3, Eq. (7), but it yields identical numerical result. In our formulation, we do not distinguish between even and odd terms, and both are conveniently summed to the same upper limit.

The first excited-state exchange interaction energy E_{ex}^1 is derived by replacing in Eq. (2) the combination

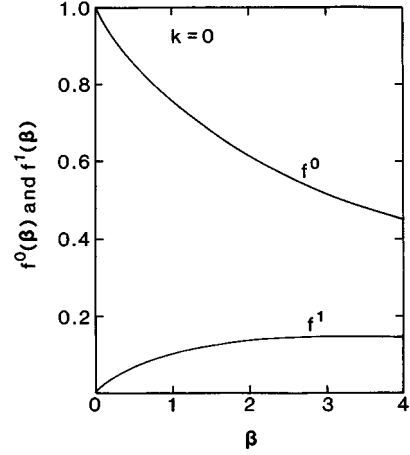


FIG. 1. Functions $f^0(\beta)$ and $f^1(\beta)$, Eqs. (6) and (7), evaluated for $k=0$.

$|\phi_0(x)|^2 |\phi_0(x')|^2$ by $\phi_0(x) \phi_1(x') \phi_0(x') \phi_1(x)$, where $\phi_1(x)$ is the excited state one-electron wave function.⁴ We choose $\phi_1(x)$ consistent with $\phi_0(x)$, with the origin at the quantum well center,

$$\phi_1(x) = \sqrt{2/L'_1} \sin(2k_1 x), \quad |x| < L'_1/2 \quad (8)$$

where $k_1 = \pi/L'_1$. For the present, we assume $L'_0 = L'_1$, that is, $k_0 = k_1$. In this approximation, the excited-state exchange interaction energy is

$$E_{\text{ex}}^1(k=0) = -\frac{e^2}{4\pi\epsilon_0} \frac{k_F}{\epsilon_r} f^1(\beta)_{k=0}, \quad (9)$$

where

$$\begin{aligned} f^1(\beta)_{k=0} &= \sum_{n=0}^{\infty} \frac{(-1)^n}{(n+1)} \frac{\beta^n}{\pi^2} \left\{ -\left(1 + \frac{1}{3^{n+1}}\right) \pi \sin(n\pi/2) \right. \\ &+ \frac{1}{2} \left(1 + 4n + \frac{11+4n}{3^{n+2}}\right) \cos(n\pi/2) \\ &+ \frac{1}{2} \sum_{k=0}^n \frac{1}{3^{k+2}} \frac{\pi^{n-k}}{(n-k)!} \left[\frac{2\pi k}{(n+1-k)} \right. \\ &\times (3 + 3^{k+2}) \sin(k\pi/2) + (7 - 3^{k+3}) \\ &\left. \left. \times \cos(k\pi/2) \right] \right\}. \quad (10) \end{aligned}$$

Figure 1 shows $f^0(\beta)_{k=0}$ and $f^1(\beta)_{k=0}$ as a function of β . The excited-state carrier interaction energy correction increases with increasing carrier concentration. The $E_{\text{ex}}^1(k=0)$ expression of Coon *et al.*, Ref. 2, Eq. (8), corresponds to the first nonvanishing term of this series, the $n=1$ term. We have also derived the exact series expression for $L'_0 \neq L'_1$. We find that for L'_0/L'_1 values of interest E_{ex}^1 become smaller. The more exact solution is very well approximated by multiplying E_{ex}^1 , Eq. (9), by the ratio of L'_0/L'_1 .

III. DIRECT COULOMB INTERACTIONS

The direct Coulomb interaction potential for the quantum well, $V_{\text{dir}}(\mathbf{r})$, is the sum of potentials due to carriers and ions,⁶

$$V_{\text{dir}}(\mathbf{r}) = V_{\text{el}}(\mathbf{r}) + V_{\text{ion}}(\mathbf{r}) \quad (11)$$

where

$$V_{\text{el}}(\mathbf{r}) = -\frac{e}{4\pi\epsilon} \sum_n \int d^3\mathbf{r}' \frac{1}{|\mathbf{r}-\mathbf{r}'|} |\psi_n(\mathbf{r}')|^2$$

and

$$V_{\text{ion}}(\mathbf{r}) = \frac{eN_D}{4\pi\epsilon} \int d^3\mathbf{r}' \frac{1}{|\mathbf{r}-\mathbf{r}'|}.$$

$V_{\text{el}}(\mathbf{r})$ is the potential at point \mathbf{r} due to carriers at position \mathbf{r}' summed over all states n , and $V_{\text{ion}}(\mathbf{r})$ is the potential due to a uniform ionized impurity density N_D . In practice, only the occupied ground state is included in calculating $V_{\text{el}}(\mathbf{r})$. For the heterolayer, \mathbf{r} is the vector sum of \mathbf{s} and x , the two-dimensional in-plane and normal to the plane coordinate vectors, respectively, and $\psi_n(\mathbf{r})$ are the basis functions.

The Coulomb direct interaction energies E_{dir}^i are

$$E_{\text{dir}}^i = -e \int d^3\mathbf{r} V_{\text{dir}}(\mathbf{r}) |\psi_i(\mathbf{r})|^2. \quad (12)$$

As in the case of exchange interactions, E_{dir}^0 and E_{dir}^1 involve well width L , doping width L_d , and ground and excited-state wave function confinement lengths L'_0 and L'_1 . Following the procedures outlined in Ref. 6, for an electrically neutral doped well,

$$E_{\text{dir}}^0 = \frac{3}{2\pi} \frac{e^2}{4\pi\epsilon_0} \frac{L'_0\sigma}{\epsilon_r} \left[1 + \frac{2}{3} \left(\frac{\pi^2}{6} - 1 \right) \left(\frac{L'_0}{L_d} - 1 \right) - \frac{\pi^2}{3} \left(1 - \frac{L_d}{L'_0} \right) \right], \quad (13)$$

and

$$E_{\text{dir}}^1 = \frac{1}{\pi} \frac{e^2}{4\pi\epsilon_0} \frac{L'_0\sigma}{\epsilon_r} \left[1 + \frac{4 \sin(a\pi)}{\pi a(4-a^2)} + \frac{1}{2} \left(\frac{L'_0}{L_d} - 1 \right) \times \left(\frac{\pi^2}{3} - \frac{1}{2} \right) a^2 - \frac{\pi^2}{2} \left(1 - \frac{L_d}{L'_0} \right) \right]. \quad (14)$$

For an isolated square well potential of finite depth and width, the upper- to ground-state confinement length ratio a is

$$a = \frac{L'_1}{L'_0} = 2 \left[\frac{E(\text{hh}_0)}{E(\text{hh}_1)} \right]^{1/2}. \quad (15)$$

Equations (13) and (14) are, to the best of our knowledge, new results. For $L'_1 = L'_0 = L_d = L$ the bracketed expressions of Eqs. (13) and (14) reduce to unity, and we obtain the equations stated in Ref. 2, Eqs. (9) and (10).

In our formulation, direct interaction effects are smaller than those derived by Coon *et al.* In the approximation, $a = L'_1/L'_0 = 1$, but $L_d \neq L'_0$, the transition energy due to direct interaction reduces to

$$E_{\text{dir}}^1(a=1) - E_{\text{dir}}^0 = -\frac{1}{4\pi} \frac{e^2}{4\pi\epsilon_0} \frac{L'_0\sigma}{\epsilon_r} \left[5 - 3 \frac{L'_0}{L_d} \right]. \quad (16)$$

For $L'_0/L_d = 1.45$, a value for a typical quantum well, our direct interaction energy shift is ~ 0.5 of that computed for $L'_0 = L_d$.

IV. RESULTS AND DISCUSSION

The carrier density adjusted transition energy E_{10} is

$$\begin{aligned} E_{10} &= E'(\text{hh}_1) - E'(\text{hh}_0) \\ &= [E(\text{hh}_1) - E(\text{hh}_0)] + [(E_{\text{dir}}^1 - E_{\text{dir}}^0) + (E_{\text{ex}}^1 - E_{\text{ex}}^0)] \\ &= \Delta E(\text{hh}) + \Delta E(\text{cc}). \end{aligned} \quad (17)$$

Here, $E'(\text{hh}_1)$ and $E'(\text{hh}_0)$ are excited- and ground-state carrier density adjusted energy levels, $\Delta E(\text{hh})$ is the intrasubband transition energy ignoring carrier interactions, and $\Delta E(\text{cc})$ is the net carrier-density-induced energy shift. We follow the formalism of Refs. 2 and 5, and add $\Delta E(\text{cc})$ as an energy correction term to $\Delta E(\text{hh})$. The E_{ex} and E_{dir} energies are derived based on penetration depths L'_0 and L'_1 , lengths computed from $E(\text{hh}_1)$ and $E(\text{hh}_0)$.

We apply the equations developed in this investigation to a p -type strained-layer $\text{Si}_{1-x}\text{Ge}_x$ quantum well deposited on a $\text{Si}(001)$ substrate. We consider the $\text{Ge}_{0.25}\text{Si}_{0.75}/\text{Si}$ composition investigated by People *et al.*⁷ Quantum well and doping widths are $L = L_d = 40$ Å, and the acceptor density is $N_A = 4 \times 10^{18} \text{ cm}^{-3}$. The infrared absorption spectra of this device is a superposition of at least four bands, two between 6–7 μm , a major band peaking near 8.0 μm , and one at ~ 10.3 μm . We calculate $E(\text{hh}_0) = 42$ meV, $E(\text{hh}_1) = 155$ meV, $L'_0 = 58$ Å, and $L'_1 = 61$ Å. These computations are based on the model of an isolated finite-depth square-well potential, the formalism developed in Ref. 8. We then find $E_{\text{ex}}^0(k=0) = -30.0$ meV, $E_{\text{ex}}^1 = -2.6$ meV, $E_{\text{dir}}^0 = 0.8$ meV, and $E_{\text{dir}}^1 = 0.3$ meV. The largest carrier density induced effect is by far due to E_{ex}^0 . The carrier density induced energy shift is $\Delta E(\text{cc}) = 27$ meV. This increases the intrasubband transition energy from 113 to 139 meV, a wavelength shift from 11.0 to 8.9 μm .

Figure 2 shows calculated ground- and excited-state exchange and direct interaction energies, and $\Delta E(\text{cc})$, as a function of N_D between 1×10^{17} and $1 \times 10^{20} \text{ cm}^{-3}$, for $x(\text{Ge}) = 0.25$ and $L = L_d = 40$ Å. Direct interaction energies increase linearly with N_D , and for large N_D the direct interaction energies and E_{ex}^1 cannot be neglected. Figure 3 shows $\Delta E(\text{cc})$ as a function of N_D for $x(\text{Ge}) = 0.25$ and $L = L_d$ ranging between 20 and 80 Å. The decreased energies at large N_D reflect the increased contributions of the direct interaction mechanism. For $L = 60$ and 80 Å, the curves are terminated at densities for which $\beta > 4$.

For large N_D , the Fermi level E_F rises above $E'(\text{hh}_1)$, the upper state is occupied, and the E_{10} transitions become forbidden. We calculate E_F , referenced to $E'(\text{hh}_0)$, from

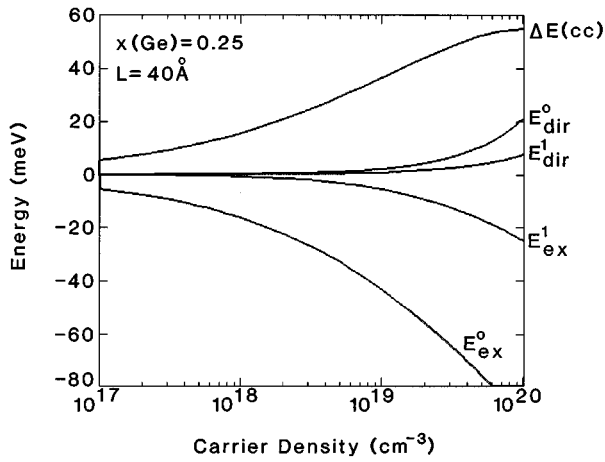


FIG. 2. Exchange and direct Coulomb interaction energies as a function of carrier density for a $\text{Ge}_{0.25}\text{Si}_{0.75}/\text{Si}$, 40-Å-wide quantum well. Superscripts 0 and 1 denote ground and excited states, respectively. $\Delta E(\text{cc})$ is the net carrier-density-induced energy shift.

$$E_F = E'(\text{hh}_0) + 2\pi(\hbar^2/2m_0)\sigma/m_{\text{hh}}. \quad (18)$$

Figures 4(a) and 4(b) show E_{10} and the transition wavelengths, respectively, for the curves depicted in Fig. 3. We terminate the curves at N_D values for which E_F equals or exceeds $E'(\text{hh}_1)$. For $L=40$ Å, this occurs at $N_D=4.5\times 10^{19}$ cm^{-3} . At this N_D , E_{10} is shifted from 113 meV for the undoped well to 164 meV for the doped well, that is, a shift from 11.0 to 7.6 μm . Figure 5 shows $\Delta E(\text{cc})$ as a function of N_D for $L=40$ Å, and $x(\text{Ge})$ between 0.2 and 0.8. $\Delta E(\text{cc})$ decreases with increasing $x(\text{Ge})$. For $N_D=1\times 10^{19}$ cm^{-3} , $\Delta E(\text{cc})$ between $x(\text{Ge})=0.2$ and $x(\text{Ge})=0.8$ varies only by 5 meV, a very small change.

Figure 6 shows E_{10} as a function of $x(\text{Ge})$ for $L=30$ Å and $N_D=0, 1\times 10^{18}$ and 1×10^{19} cm^{-3} . Transition energies increase with N_D . Energy shifts between the undoped and the 1×10^{19} cm^{-3} doped quantum wells range between 31 and 38 meV. The curves show a sharp break at $x(\text{Ge})=0.19$. This is the $x(\text{Ge})$ composition at which $E'(\text{hh}_1)$ rises above the barrier edge into the continuum, and it defines the intersection of bound-to-bound transitions and bound-to-

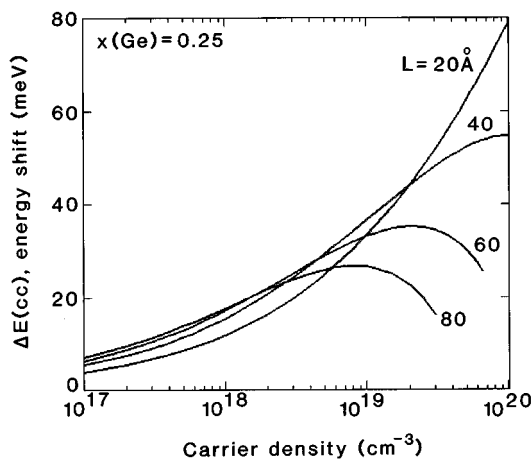


FIG. 3. Carrier-density-induced energy shift as a function of carrier density and well width for a $\text{Ge}_{0.25}\text{Si}_{0.75}/\text{Si}$ quantum well.

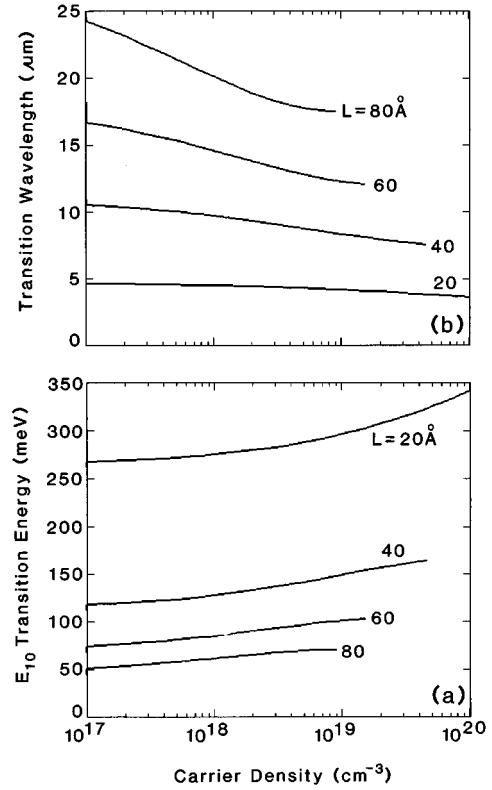


FIG. 4. (a) Carrier-density-adjusted transition energy E_{10} as a function of carrier density and width for a $\text{Ge}_{0.25}\text{Si}_{0.75}\text{Si}$ quantum well. (b) Corresponding transition wavelengths.

continuum resonances. The conditions for transmission resonances are discussed by Bastard.^{9,10} Wang and Karunasiri assert that for infrared-photodetector applications, the most efficient device configuration is for the first excited state to be close to the valence subband barrier edge.¹¹ For a wider $L=40$ Å well, $E'(\text{hh}_1)$ is bound, and E_{10} increases monotonically with $x(\text{Ge})$.

Figure 7 shows $\Delta E(\text{cc})$ as a function of L for $x(\text{Ge})=0.25$ and N_D between 1×10^{17} and 1×10^{19} cm^{-3} . $\Delta E(\text{cc})$ exhibits a peak, which shifts with increasing N_D to smaller L . Figure

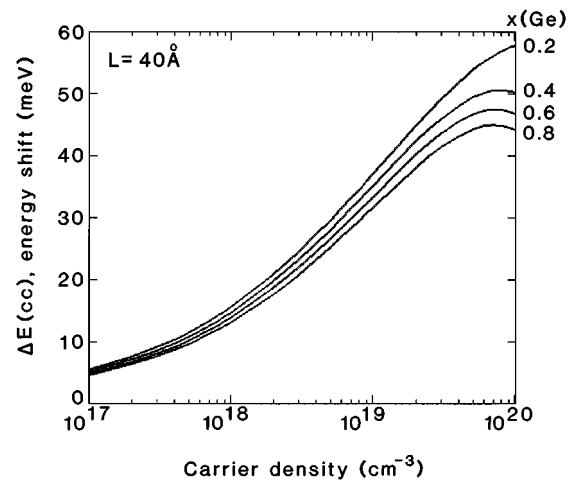


FIG. 5. Carrier-density-induced energy shift as a function of carrier density and Ge composition for $\text{Si}_{1-x}\text{Ge}_x/\text{Si}$ quantum wells.

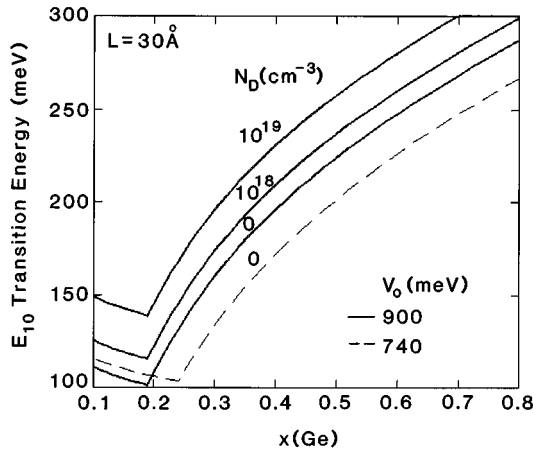


FIG. 6. Transition energy of $\text{Si}_{1-x}\text{Ge}_x/\text{Si}$ quantum wells as a function of Ge composition and carrier density. For $x(\text{Ge}) < 0.19$, E_{10} are bound-to-continuum resonances, and for $x(\text{Ge}) > 0.19$, E_{10} are bound-to-bound transitions. V_0 is the heavy-hole valence subband offset between the pseudomorphically strained Ge and relaxed Si substrate.

8 illustrates E_{10} as a function of L and L_d . In typical applications, L_d/L ranges between 0.5 and 0.75, and maximum E_{10} shifts between fully and partially doped quantum well widths are less than 5 meV. We also find that $x(\text{Ge})$ variations of the transition energy with L_d/L are insignificant, less than 5 meV. However, L_d/L effects can become significant for narrow doping widths.

One issue complicating data comparison with calculated E_{10} is the value assumed for $V_0(\text{Ge/Si})$, the valence heavy-hole subband offset between the pseudomorphically strained Ge and the relaxed Si substrate. Theoretical and experimental values range between 730 and 900 meV. In our calculations we used the van der Walls recommended value of 900 meV.¹² In Fig. 6, the dashed line shows $\Delta E(\text{hh})$ using $V_0(\text{Ge/Si}) = 740$ meV. In the bound-to-continuum region E_{10} differences between the two V_0 values are small, but for bound-to-bound transitions the shallower potential well reduces E_{10} by ~ 25 meV. Consequently, in fitting data one should be cognizant of the fact that an arbitrary choice of

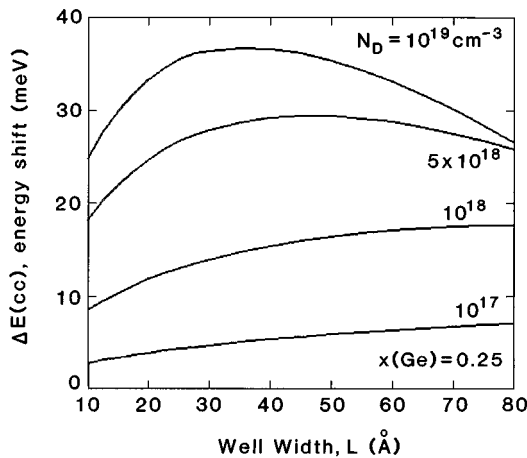


FIG. 7. Carrier-density-induced energy shift as a function of well width and carrier density for a $\text{Ge}_{0.25}\text{Si}_{0.75}/\text{Si}$ quantum well.

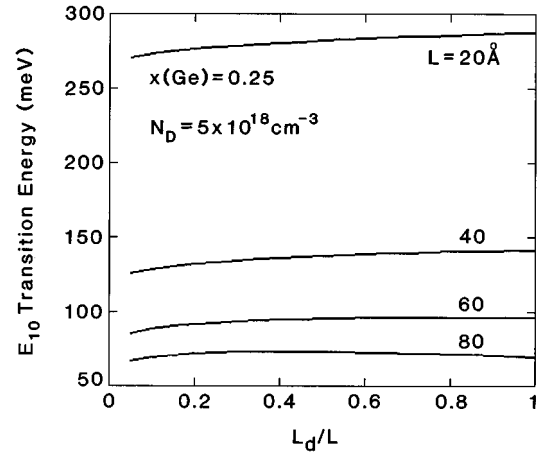


FIG. 8. Transition energy as a function of doping width L_d and well width L for a carrier-doped $\text{Ge}_{0.25}\text{Si}_{0.75}/\text{Si}$ quantum well. For large L_d/L , E_{10} differences between fully and partially doped quantum wells are small.

$V_0(\text{Ge/Si})$ can reduce computed transition energies, thus offsetting $\Delta E(\text{cc})$ effects. For the previously cited $x(\text{Ge}) = 0.25$, $L = 40$ Å quantum well, the $V_0(\text{Ge/Si})$ change from 900 to 740 meV reduces $\Delta E(\text{hh})$ by 13 meV.

In general, the infrared spectra of $\text{Si}_{1-x}\text{Ge}_x/\text{Si}$ quantum wells are superpositions of interband, e.g., heavy-hole to light-hole, and intrasubband, e.g., heavy-hole to heavy-hole, transition peaks and free-carrier absorption. Zanier *et al.* show that peak position values are strongly affected by the method utilized in subtracting the free-carrier background.^{13,14} In their approach, the peak position is a fitted parameter, derived from the best fit to a model of free-carrier absorption and a Lorentzian peak. This problem is also discussed by Kreifels *et al.*, and they advocate a self-reference technique.¹⁵ Zanier *et al.* report spectra for three $L = 30$ Å quantum wells (i) $x(\text{Ge}) = 0.2$, $N_D = 2 \times 10^{18}$, (ii) $x(\text{Ge}) = 0.2$, $N_D = 2 \times 10^{19}$, and (iii) $x(\text{Ge}) = 0.3$, $N_D = 2 \times 10^{18}$ cm^{-3} . Well compositions are approximate, and energy peaks are broad. Fitted E_{10} peak positions for samples (i), (ii), and (iii), are ~ 115 , ~ 125 , and ~ 160 meV, respectively. Our calculated values are 122, 151, and 170 meV. For $x(\text{Ge}) = 0.2$, the relative energy difference between the two N_D samples is 10 meV, and our calculated value is 29 meV. For $N_D = 2 \times 10^{18}$ cm^{-3} , the relative energy difference between the two $x(\text{Ge})$ samples is 45 meV, and our calculated value is 48 meV. Sample $x(\text{Ge}) = 0.2$ is just at the intersection of bound-to-bound and bound-to-continuum transitions, and a slight shift in a parameter drastically affects experimental and calculated E_{10} .

In a series of publications Wang and co-workers reported infrared measurements of $\text{Si}_{1-x}\text{Ge}_x/\text{Si}$ quantum wells.¹⁶⁻²⁰ Many of these results are summarized in Ref. 11. In these publications, the free-carrier absorption subtraction method is unspecified. For $N_D = 1 \times 10^{19}$ cm^{-3} , E_{10} peaks for $x(\text{Ge})$ compositions 0.15, 0.40, and 0.50 are at ~ 145 , ~ 153 , and ~ 172 meV.¹⁶⁻¹⁸ Our calculated values are 143, 176, and 190 meV. The $x(\text{Ge}) = 0.15$ quantum well is a bound-to-continuum type transition. The measured energy shift between $x(\text{Ge}) = 0.4$ and 0.5 is 19 meV, and our computed value is 14 meV. For $N_D = 5 \times 10^{19}$ cm^{-3} , $L = 40$ Å, and

$L_d=30 \text{ \AA}$, measured values of E_{10} for $x(\text{Ge})=0.4$ and 0.60 are ~ 220 and ~ 234 meV, respectively.^{19,20} Our calculated values of E_{10} are 200 and 223 meV. For these samples the relative measured and calculated energy shifts are 14 and 23 meV, respectively. In general, differences between measured and calculated E_{10} are within 25 meV.

V. CONCLUSIONS

We have evaluated Coulomb carrier-carrier exchange and direct interaction effects for the heavy-hole subband of strained-layer quantum wells. We have derived, in a consistent manner, the associated energy shifts both for the ground- and the excited-states. Ground- and excited-state exchange interaction energies, E_{ex}^0 and E_{ex}^1 , are negative, whereas ground- and excited-state direct interaction energies, E_{dir}^0 and E_{dir}^1 , are positive. The net carrier density induced energy shift is a balance between these positive and negative offsets. In deriving these energy expressions we follow, and extend, the formalism of Coon *et al.*¹⁻⁶ For E_{ex}^0 we reproduce their results. In deriving E_{ex}^1 , these investigators approximated an

exponential by the first nonzero term of its power series expansion. Our results for E_{ex}^1 are based on the complete expansion of the exponential. We find, in agreement with these investigators, that E_{ex}^1 is substantially smaller than E_{ex}^0 . For E_{dir}^0 and E_{dir}^1 , we consider an electrically neutral doped well. In our derivation we differentiate between well width, ground- and excited-state wave function confinement lengths, and doping layer width. Our results for E_{dir}^0 and E_{dir}^1 yield substantially smaller energy shifts than the ones given by Coon *et al.* Consequently, for small carrier densities E_{ex}^0 is the primary component of many-body effects. However, direct interaction energies increase linearly with carrier density, and for large carrier densities do become important and substantially negate exchange interaction effects.

ACKNOWLEDGMENTS

The authors thank M. Shatz of MIT, Lincoln Laboratory, and our colleagues G. Sun, M. Chi, and A. Anselmo at Rome Laboratory for comments and discussions.

-
- ¹K. M. S. V. Bandara and D. D. Coon, *Appl. Phys. Lett.* **53**, 1865 (1988).
- ²K. M. S. V. Bandara, D. D. Coon, Byung-sung O, Y. F. Lin, and M. H. Francombe, *Appl. Phys. Lett.* **53**, 1931 (1988).
- ³J.-W. Choe, Byung-sung O, K. M. S. V. Bandara, and D. D. Coon, *Appl. Phys. Lett.* **56**, 1679 (1990).
- ⁴J.-W. Choe, Byung-sung O, K. M. S. V. Bandara, and D. D. Coon, *Superlattices Microstruct.* **10**, 1 (1991).
- ⁵D. D. Coon and K. M. S. V. Bandara, in *Physics of Thin Films*, edited by M. H. Francombe and J. L. Vossen (Academic, Boston, 1991), p. 219.
- ⁶S. V. Bandara, Ph.D. thesis, University of Pittsburgh, 1988.
- ⁷R. People, J. C. Bean, C. G. Bethea, S. P. Sputz, and L. J. Petricolas, *Appl. Phys. Lett.* **61**, 1122 (1992).
- ⁸A. Kahan, M. Chi, and L. Friedman, *J. Appl. Phys.* **75**, 8012 (1994).
- ⁹G. Bastard, *Wave Mechanics Applied to Semiconductor Heterostructures* (Halsted, New York, 1988), p. 93.
- ¹⁰G. Bastard, J. A. Brum, and R. Ferreira, in *Solid State Physics*, edited by H. Ehrenreich and D. Turnbull (Academic, Boston, 1991), Vol. 44, p. 250.
- ¹¹K. L. Wang and R. P. G. Karunasiri, in *Semiconductor Quantum Wells and Superlattices for Long-Wavelength Infrared Detectors*, edited by M. O. Manasreh (Artech House, Norwood, MA, 1993), p. 152.
- ¹²C. G. Van de Walle, *Phys. Rev. B* **39**, 1871 (1989).
- ¹³S. Zanier, J. M. Berroir, Y. Guldner, J. P. Vieren, I. Sagnes, F. Glowacki, Y. Campidelli, and P. A. Badoz, *Phys. Rev. B* **51**, 14 311 (1995).
- ¹⁴J. M. Berroir, S. Zanier, Y. Guldner, J. P. Vieren, I. Sagnes, Y. Campidelli, and P. A. Padoz, *Appl. Surf. Sci.* **102**, 331 (1996).
- ¹⁵T. L. Kreifels, R. L. Hengehold, Y. K. Yeo, P. E. Thompson, and D. S. Simons, *J. Vac. Sci. Technol. A* **13**, 636 (1995).
- ¹⁶R. P. G. Karunasiri, J. S. Park, and K. L. Wang, *Appl. Phys. Lett.* **59**, 2588 (1991).
- ¹⁷R. P. G. Karunasiri, J. S. Park, Y. J. Mii, and K. L. Wang, *Appl. Phys. Lett.* **57**, 2585 (1990).
- ¹⁸J. S. Park, Ph.D. thesis, UCLA, 1992, p. 61.
- ¹⁹J. S. Park, R. P. G. Karunasiri, and K. L. Wang, *Appl. Phys. Lett.* **61**, 681 (1992).
- ²⁰R. P. G. Karunasiri, *Jpn. J. Appl. Phys.* **33**, 1468 (1994).